Published in Journal of Polymer Research (Accepted 2007)
http://dx.doi.org/10.1007/s10965-007-9154-2

A modeling approach for prediction of erosion behavior of glass fiber–polyester composites

Amar Patnaik · Alok Satapathy · S. S. Mahapatra · R. R. Dash

Abstract In recent years, a fairly good number of articles dealing in characterization of solid particle erosion of glass fiber reinforced composites are available but exhaustive study on this vital aspect leading to understand erosion phenomenon is hardly found in the literature. Therefore, in the present work, a theoretical model based on principle of conservation of particle kinetic energy is developed to determine wear rate of glass–polyester composites due to multiple impact erosion. Room temperature erosion tests are then carried out to study the effect of various control factors in an interacting environment on the erosion behavior of these composites. For this purpose, design of experiments approach utilizing Taguchi's orthogonal arrays is adopted to test the specimens on air jet type erosion test configuration. The results indicate that erodent size, fiber loading, impingement angle and impact velocity are the significant factors in the order of their influence on wear rate. Taguchi approach enables to determine optimal parameter settings that lead to minimization of erosion rate. Artificial neural network (ANN) approach is applied to the erosive wear data to reach at acceptable predictive models. Scanning electron microscopy of the eroded surface of the composites is performed for observation of the features such as crack formation, fiber fragmentation and matrix body deformation. Finally, popular evolutionary approach known genetic algorithm (GA) is used to generalize the method of finding out optimal factor settings for minimum wear rate.

Keywords Erosion modeling · Polyester composite; Taguchi design · ANN · GA

A. Patnaik (✉)
Mechanical Engineering, N.I.T. Hamirpur,
Hamirpur, Himachal Pradesh, 177005, India
e-mail: amar_mtech@rediffmail.com

A. Satapathy · S. S. Mahapatra
Mechanical Engineering, N.I.T. Rourkela,
Rourkela, Orissa, 769008, India

R. R. Dash
Mechanical Engineering,
Gandhi Institute of Engineering and Technology,
Gunupur, Orissa, India

Introduction

Solid particle erosion is a general term used to describe mechanical degradation (wear) of any material subjected to a stream of erodent particles impinging on its surface. The effect of solid particle erosion has been recognized by many researchers Wahl and Hartenstein [1] for a long time. Damage caused by erosion has been reported in several industries for a wide range of situations. Examples have been sited for transportation of airborne solids through pipes by Bitter [2], boiler tubes exposed to fly ash by Raask [3] and gas turbine blades by Hibbert and Roy [4]. Solid particle erosion is the progressive loss of original material from a solid surface due to mechanical interaction between that surface and solid particles. Various applications of polymers and their composites in erosive wear situations are reported by Pool et al. [5], Kulkarni and Kishore [6] and Ruff and Ives [7] in the literature. But solid particle erosion of polymers and their composites have not been investigated to the same extent as for metals or ceramics. However, a number of researchers Barkoula and Karger-Kocsis [8], Tewari et al. [9] have evaluated the resistance of various types of polymers and their composites to solid particle erosion. It is widely recognized that polymer and their composites have poor erosion resistance. Their erosion rates (E_r) are considerably higher than metals. Also, it is

well known that the erosion rate of polymer composites is even higher than that of neat polymers as reported by Häger et al. [10]. The solid particle erosion behavior of polymer composites as a function of fiber content has been studied to a limited extent by investigators like Miyazaki and Takeda [11]. Tilly and Sage [12] have investigated the influence of velocity, impact angle, particle size and weight of impacted abrasives on nylon, carbon–fiber-reinforced nylon, epoxy resin, polypropylene and glass–fiber-reinforced plastic.

Lindsley and Marder [13] found impact velocity (v) to be a critical test variable in erosion, and that it can easily over shadow changes in other variables, such as target material, impact angle etc. Sundararajan and Manish [14] suggested that in addition to velocity, solid particle erosion is governed by the impact angle, particle size, particle shape and hardness. The impact of above parameters has been studied independently keeping all parameters at fixed levels. Therefore, visualization of impact of various factors in an interacting environment really becomes difficult. To this end, an attempt has been made to analyze the impact of more than one parameter on solid particle erosion of PMCs, because in actual practice the resultant erosion rate is the combined effect of impact of more than one interacting variables. An inexpensive and easy-to-operate experimental strategy based on Taguchi's parameter design has been adopted to study effect of various parameters and their interactions. The experimental procedure has been successfully applied by Mahapatra and Patnaik [15, 16, 17, 18, 19, 20, 21] for parametric appraisal in wire electrical discharge machining (WEDM) process, drilling of metal matrix composites, and erosion behavior of metal matrix composites such as aluminium reinforced with red mud.

The aim of the present study is, therefore, to investigate the erosion behavior of polyester matrix composites based on Taguchi method under various testing conditions. Further more, the analysis of variance are employed to investigate the most significant control factors and their interactions. Finally, evolutionary approach known as genetic algorithm has been applied for optimal factor settings to minimize the erosion rate.

Mathematical model

Nomenclature

The following symbols are used in this paper:

r	Chord length of the indentation (m)
d	Erodent diameter (m)
δ	Indentation depth (m)
e_v	Volumetric wear loss per particle impact (m^3)
E_V	Total volumetric erosion wear rate (m^3/s)
α	Angle of impingement (degree)
V	Impact velocity (m/s)
P	Force on the indenter (N)
H_v	Hardness (N/m^2)
m	Mass of single erodent particle (kg)
M	Mass flow rate of the erodent (kg/s)
N	Number of impact per unit time (s^{-1})
ρ_c	Density of composite (kg/m^3)
ρ	Density of erodent (kg/m^3)
η_{normal}	Erosion efficiency with normal impact
η	Erosion efficiency
E_{rth}	Erosion wear rate (kg/kg)

Solid particle erosion is a wear process in which the material is removed from a surface by the action of a high velocity stream of erodent particles entrained in a high velocity fluid stream. The particles strike against the surface and promote material loss. During flight, a particle carries momentum and kinetic energy which can be dissipated during the impact due to its interaction with a target surface. As far as erosion study of polymer matrix composites is concerned, no specific model has been developed and thus the study of their erosion behavior has been mostly experimental. However, Mishra [22] proposed a mathematical model for material removal rate in abrasive jet machining process in which the material is removed from the work piece in a similar fashion. This model assumes that the volume of material removed is same as the volume of indentation caused by the impact. This has a serious limitation as in a real erosion process the volume of material removed is actually different from the indentation volume. Further, this model considers only the normal impact i.e. $\alpha=90°$ whereas in actual practice, particles may impinge on the surface at any angle ($0°\leq\alpha\leq 90°$). The proposed model addresses these shortcomings in an effective manner. It considers the real situation in which the volume of material removed by erosion is not same as the volume of material displaced and therefore, additional term "erosion efficiency (η)" is incorporated in the erosion wear rate formulation. In the case of a stream of particles impacting a surface normally (i.e. at $\alpha=90°$), erosion efficiency (η_{normal}) defined by Sundararajan and Manish [14] is given as

$$\eta_{\text{normal}} = \frac{2E_r H_v}{\rho V^2} \tag{1}$$

But considering impact of erodent at any angle α to the surface, the actual erosion efficiency can be obtained by modifying Eq. 1 as

$$\eta = \frac{2E_r H_v}{\rho V^2 \sin^2\alpha} \tag{2}$$

The model is based on the assumption that the kinetic energy of the impinging particles is utilized to cause micro-

indentation in the composite material and the material loss is a measure of the indentation. The erosion is the result of cumulative damage of such non-interacting, single particle impacts. The model further assumes the erodent particles to be rigid, spherical bodies of diameter equal to the average grit size. It considers the ductile mode of erosion and assumes the volume of material lost in a single impact is less than the volume of indentation. The model is developed with the simplified approach of energy conservation which equals the erodent kinetic energy with the work done in creating the indentation.

The model for ductile mode erosion proceeds as follows. From the geometry of Fig. (1), $r^2 = d \times \delta$

$$\text{The volume of indentation} = \pi\delta^2\left[\frac{d}{2} - \frac{\delta}{3}\right]$$

So, the volumetric wear loss per particle impact is given by

$$e_v = \text{Volume of indentation} \times \eta$$

$$= \eta \times \pi\delta^2\left[\frac{d}{2} - \frac{\delta}{3}\right] \text{and neglecting } \delta^3 \text{ terms}$$

$$= \frac{\pi \times d \times \delta^2}{2} \times \eta$$

Considering N number of particle impacts per unit time, the volumetric erosion wear loss will be

$$E_V = \frac{\pi \times d \times \delta^2}{2} N \times \eta \tag{3}$$

The impact velocity will have two components; one normal to the composite surface and one parallel to it. At zero impact angles, it is assumed that there is negligible wear because eroding particles do not practically impact the target surface [8]. Consequently, there will be no erosion due to the parallel component and the indentation is assumed to be caused entirely by the component normal to the composite surface as shown in Fig. (2).

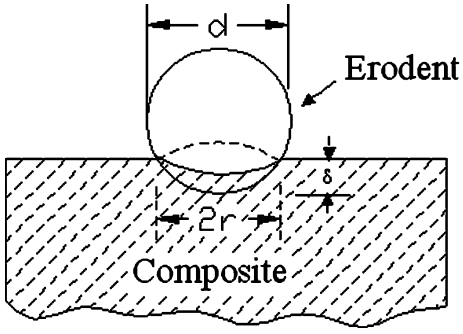

Fig. 1 Scheme of material removal mechanism in ductile mode

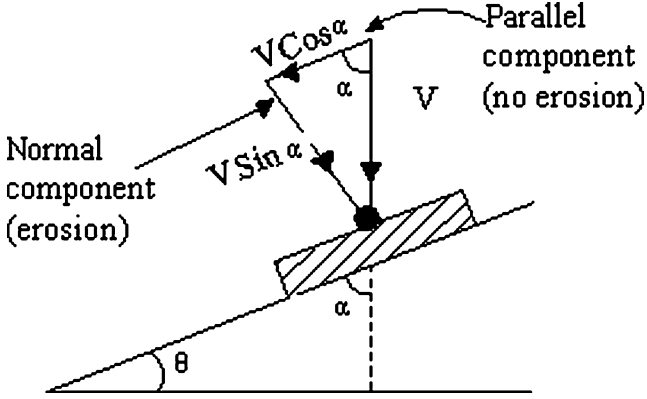

Fig. 2 Resolution of impact velocity in normal and parallel directions

Now applying conservation of energy to the single impact erosion process, kinetic energy associated with the normal velocity component of a single erodent particle is equal to the work done in the indentation of composite. The energy of impact introduces a force P on the indenter to cause the indentation in the composite. Thus,

$$\frac{1}{2} m v^2 \sin^2\alpha = \frac{1}{2} \times P \times \delta \tag{4}$$

So,

$$\frac{1}{2}\left(\frac{\pi d^3}{6}\right)\rho\, v^2 \sin^2\alpha = \frac{1}{2}\left(\pi r^2 H_V\right)\delta$$

On solving;

$$\delta^2 = \frac{\rho \times V^2 d^2 \sin^2\alpha}{6H_V} \tag{5}$$

The number of erodent particle impacting the target is estimated from the known value of erodent mass flow rate, M as

$$N = \frac{M}{\frac{\pi d^3}{6}\rho} \tag{6}$$

Substituting the value of δ in Eq. 3

$$E_V = \frac{\pi \times d \times d^2 \times V^2 \times \sin^2\alpha \times \rho}{2 \times 6H_V} \times \frac{M \times 6}{\pi \times d^3 \rho} \times \eta$$

$$E_V = \frac{V^2 \times \sin^2\alpha}{2H_V} \times \eta$$

Erosion rate (E_r) defined as the ratio of mass lost due to erosion to the mass of erodent is now expressed as.

$$E_r = \frac{\rho_c \times \eta \times V^2 \times \sin^2\alpha}{2H_V} \tag{7}$$

Material removal by impact erosion wear involves complex mechanisms. A simplified theoretical model for such a

process may appear inadequate unless its assessment against experimental results is made. So for the validation of the proposed model erosion tests on the composites are conducted at various operating conditions.

Experimental program

Materials

Cross plied E-glass fibers (360 roving taken from Saint Govion) are reinforced in unsaturated isophthalic polyester resin (supplied by Ciba-Giegy Ltd. India) to prepare the composites. The composite slabs are made by conventional hand-lay-up technique. Two percent cobalt nephthalate (as accelerator) is mixed thoroughly in isophthalic polyester resin and then 2% methyl–ethyl–ketone–peroxide (MEKP) as hardener is mixed in the resin prior to reinforcement. E-glass fiber and polyester resin have modulus of 72.5 and 3.25 GPa respectively and possess density of 2.59 and 1.35 gm/cc respectively. Three composites of different glass fiber weight fractions (30, 40 and 50 wt.%) are fabricated. The castings are put under load for about 24 h for proper curing at room temperature. Specimens of suitable dimension are cut using a diamond cutter for mechanical characterization and erosion test.

Test apparatus

The room temperature erosion test facility used in the present investigation is illustrated schematically in Fig. 3. The set up is capable of creating reproducible erosive situation for assessing erosion wear resistance of the prepared composite samples. The conditions (confirming to ASTM G 76 test standards) under which erosion tests are carried out are listed in Table 1. Dry silica sand (density 2.5 gm/cc) is used as the erodent. The particles fed at constant rate are made to flow with compressed air jet to impact the specimen, which can be held at various angles with respect to the flow direction of erodent using a swivel

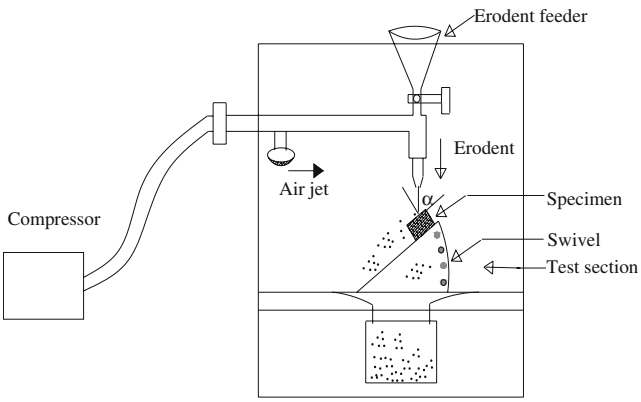

Fig. 3 A schematic diagram of the erosion rig

Table 1 Parameters of the setting

Control factors	Symbols	Fixed parameters	
Velocity of impact	Factor *A*	Erodent	Silica sand
Fiber loading	Factor *B*	Erodent feed rate (g/min)	10.0±1.0
Stand-off distance	Factor *C*	Test temperature	RT
Impingement angle	Factor *D*	Nozzle diameter (mm)	3
Erodent size	Factor *E*	Length of nozzle (mm)	80

and an adjustable sample clip. The velocity of the eroding particles is determined using double disc method [7]. The samples were cleaned in acetone, dried and weighed to an accuracy of ±0.1 mg accuracy using a precision electronic balance. These are then eroded in the test rig for 10 min and weighed again to determine the weight loss. The procedure is repeated till the erosion rate attains a constant value called steady state erosion rate. The ratio of this weight loss to the weight of the eroding particles causing the loss (i.e. testing time × particle feed rate) is then computed as the normalized erosion rate.

Mechanical characterization

Micro-hardness measurement is done using a Leitz micro-hardness tester equipped with a square based pyramidal (angle 136° between opposite faces) diamond indenter by applying a load of 24.54 N. The tensile test is performed on flat dog-bone shaped composite specimens as per ASTM D 3039-76 test standards an universal testing machine Instron 1195. Three point bend test is conducted in the same machine at across head speed of 10 mm/min to evaluate the flexural strength of the composites. Finally, the eroded surfaces of some selected samples are examined by scanning electron microscope JEOL JSM-6480LV.

Experimental design

Design of experiment is a powerful analysis tool for modeling and analyzing the influence of control factors on performance output. The most important stage in the design of experiment lies in the selection of the control factors. Therefore, a large number of factors are included so that non-significant variables can be identified at earliest opportunity. The operating conditions under which erosion tests were carried out are given in Table 2. The tests were conducted as per experimental design given in Table 3 under room temperature.

Five parameters viz., impact velocity, fiber loading, stand-off distance, impingement angle and erodent size, each at

Table 2 Levels for various control factors

Control factor	Level			
	I	II	III	Units
A: Velocity of impact	32	45	58	m/s
B: Fiber loading	30	40	50	%
C: Stand-off distance	120	180	240	Mm
D: Impingement angle	30	60	90	degree
E: Erodent size	300	500	800	μm

three levels, are considered in this study in accordance with L_{27} (3^{13}) orthogonal array design. In Table 3, each column represents a test parameter and a row gives a test condition which is nothing but combination of parameter levels. Five parameters each at three levels would require 3^5=243 runs in a full factorial experiment. Whereas, Taguchi's factorial experiment approach reduces it to 27 runs only offering a great advantage.

The experimental observations are transformed into a signal-to-noise (*S*/*N*) ratio. There are several *S*/*N* ratios available depending on the type of characteristics. The *S*/*N* ratio for minimum erosion rate coming under smaller is better characteristic, which can be calculated as logarithmic transformation of the loss function as shown below.

Smaller is the better characteristic :

$$\frac{S}{N} = -10 \log \frac{1}{n}\left(\sum y^2\right) \tag{8}$$

where n the number of observations, and y the observed data. "Lower is better" (LB) characteristic, with the above *S*/*N* ratio transformation, is suitable for minimizations of erosion rate. The standard linear graph by Glen [23] and Madhav [24], as shown in Fig. 4, is used to assign the factors and interactions to various columns of the orthogonal array. Solid particle erosion is characterized by a large number of factors such as impact velocity, fiber loading, stand off-distance, impingement angle, and erodent size. Out of all these factors, velocity predominantly governs the rate of erosion.

The plan of the experiments is as follows: the first column was assigned to impact velocity (*A*), the second column to fiber loading (*B*), the fifth column to stand-off distance (*C*), the ninth column to impingement angle (*D*) and tenth column to erodent size (*E*), the third and fourth column are assigned to $(A\times B)_1$ and $(A\times B)_2$, respectively to

Table 3 Orthogonal array for L_{27} (3^{13}) Taguchi design

$L_{27}(3^{13})$	1 *A*	2 *B*	$3(A\times B)_1$	$4(A\text{x}B)_2$	5 *C*	$6(B\times C)_1$	$7(B\times C)_2$	$8(A\times C)_1$	9 *D*	10 *E*	$11(A\times C)_2$	12	13
1	1	1	1	1	1	1	1	1	1	1	1	1	1
2	1	1	1	1	2	2	2	2	2	2	2	2	2
3	1	1	1	1	3	3	3	3	3	3	3	3	3
4	1	2	2	2	1	1	1	2	2	2	3	3	3
5	1	2	2	2	2	2	2	3	3	3	1	1	1
6	1	2	2	2	3	3	3	1	1	1	2	2	2
7	1	3	3	3	1	1	1	3	3	3	2	2	2
8	1	3	3	3	2	2	2	1	1	1	3	3	3
9	1	3	3	3	3	3	3	2	2	2	1	1	1
10	2	1	2	3	1	2	3	1	2	3	1	2	3
11	2	1	2	3	2	3	1	2	3	1	2	3	1
12	2	1	2	3	3	1	2	3	1	2	3	1	2
13	2	2	3	1	1	2	3	2	3	1	3	1	2
14	2	2	3	1	2	3	1	3	1	2	1	2	3
15	2	2	3	1	3	1	2	1	2	3	2	3	1
16	2	3	1	2	1	2	3	3	1	2	2	3	1
17	2	3	1	2	2	3	1	1	2	3	3	1	2
18	2	3	1	2	3	1	2	2	3	1	1	2	3
19	3	1	3	2	1	3	2	1	3	2	1	3	2
20	3	1	3	2	2	1	3	2	1	3	2	1	3
21	3	1	3	2	3	2	1	3	2	1	3	2	1
22	3	2	1	3	1	3	2	2	1	3	3	2	1
23	3	2	1	3	2	1	3	3	2	1	1	3	2
24	3	2	1	3	3	2	1	1	3	2	2	1	3
25	3	3	2	1	1	3	2	3	2	1	2	1	3
26	3	3	2	1	2	1	3	1	3	2	3	2	1
27	3	3	2	1	3	2	1	2	1	3	1	3	2

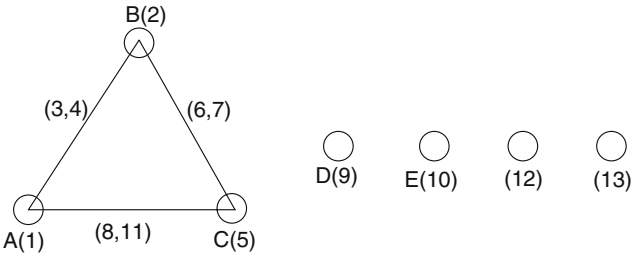

Fig. 4 Standard linear graphs for L_{27} array

estimate interaction between impact velocity (A) and fiber loading (B), the sixth and seventh column are assigned to $(B\times C)_1$ and $(B\times C)_2$ respectively, to estimate interaction between the fiber loading (B) and stand-off distance (C), the eighth and eleventh column are assigned to $(A\times C)_1$ and $(A\times C)_2$ respectively, to estimate interaction between the impact velocity (A) and stand-off distance (C). The remaining columns are assigned to error columns respectively.

Results and discussion

Mechanical properties

Figure 5 shows the micro-hardness values for different compositions. It is seen that with the increase in fiber content in the composite, its hardness value improves although the increment is marginal. Figures 6 and 7 show the variation of tensile and flexural strengths of the composites with the fiber content. A gradual increase in tensile strength as well as flexural strength with the weight fraction of fiber is noticed. It clearly indicates that inclusion of glass fiber improves the load bearing capacity and the ability to withstand bending of the composites. Similar observations have been reported by Harsha et al. [25] for other fiber reinforced thermoplastics such as polyaryletherketone composites. It may be mentioned here that both tensile and flexural strengths are important for recommending any composite as a candidate for structural applications.

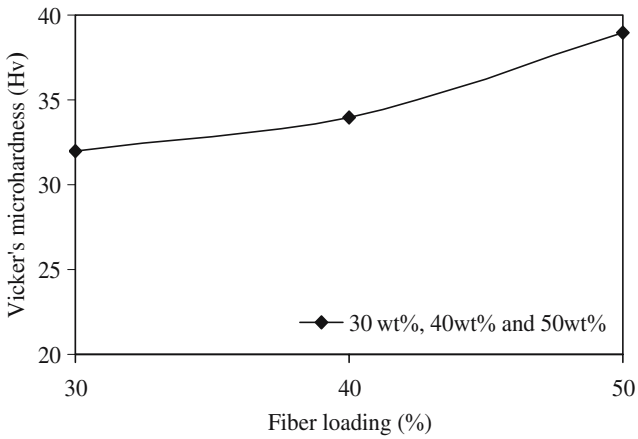

Fig. 5 Variation of microhardness vs. fiber loading

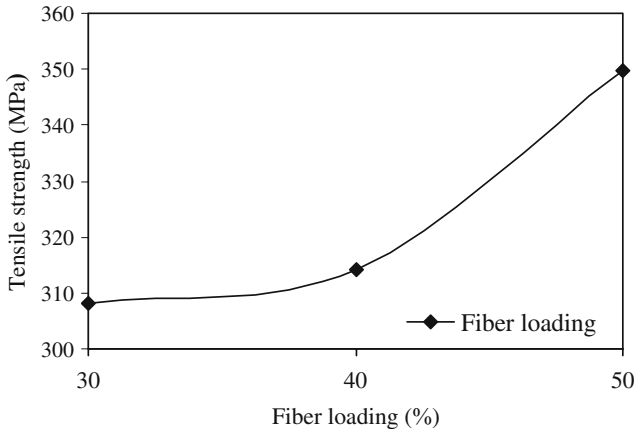

Fig. 6 Effect of fiber loading on tensile strength of glass fiber polyester composites

Steady state erosion

Erosion wear behavior of materials can be grouped as ductile and brittle categories although this grouping is not definitive. Thermoplastic matrix composites usually show ductile behavior and have the peak erosion rate at around 30° impact angle because cutting mechanism is dominant in erosion. While the thermosetting ones erode in a brittle manner with the peak erosion occurring at normal impact. However, there is a dispute about this failure classification as the erosive wear behavior depends strongly on the experimental conditions and the composition of the target material [8]. Figure 8 shows the impact angle dependence of the erosion rate of polyester composites with different fiber content. The curves are plotted with the results of erosion tests conducted for different impingement angle keeping all other parameters constant (impact velocity= 32 m/s, stand-off distance=120 mm and erodent size=

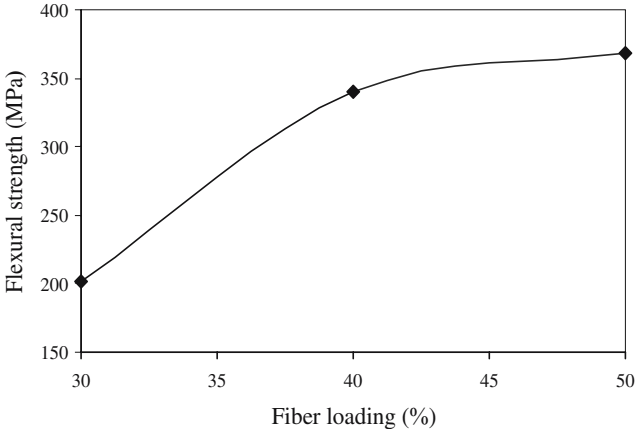

Fig. 7 Effect of fiber loading on flexural strength of glass fiber polyester composites

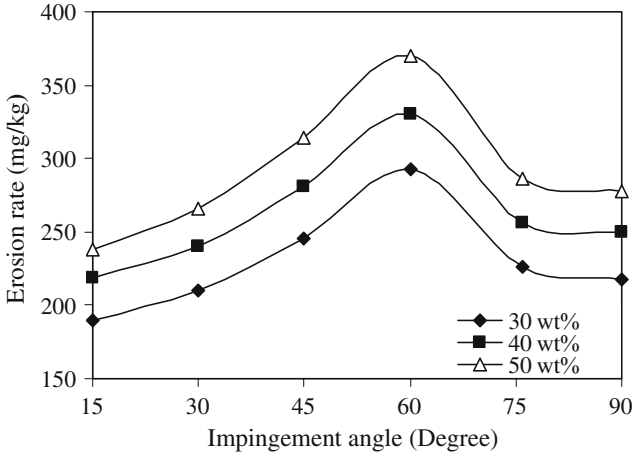

Fig. 8 Erosion rate vs. Angle of impingement for different fiber loading

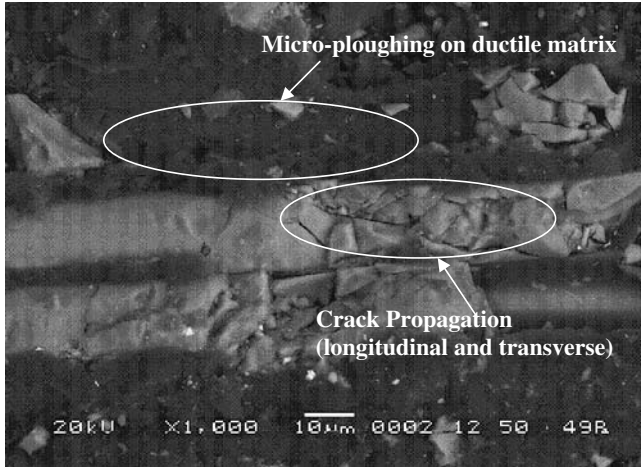

Fig. 10 SEM micrograph (× 1,000) of GF Polymer composite eroded surface (impact velocity 58 m/s, fiber loading 50%, S.O.D 120 mm, impingement angle 60° and erodent size 300 μm)

300 μm). It can be seen that the peaks of erosion rates are located at an angle of 60° for all the samples irrespective of fiber content. This shows semi-ductile erosion behavior of the composite. It is further noted (Fig. 8) that the erosion rate increases with increase in fiber content. Sundararajan et al. [26] concluded that this behavior is attributed to the fact that the harder the material, larger is the fraction of the crater volume that is removed. In this investigation higher hardness values have been noted for composites with higher fiber loading and this is therefore the reason why the composites exhibit declining erosion resistance with the increase in fiber content.

To identify the mode of material removal, the morphologies of eroded surfaces are observed under scanning electron microscope. Figure 9 shows the local removal of resin material from the impacted surface resulting in exposure of the fibers to the erodent flux. This micrograph also reveals that due to sand particle impact on fibers there is formation of transverse cracks that break these fibers. Figure 10 presents the microstructure of the composite eroded at high impact velocity (58 m/s), at lower stand-off distance (120 mm) and at an impingement angle of 60°. Here the propagation of crack along transverse as well as longitudinal direction is well visualized. On comparing this micro-structure with that of the same composite eroded at a lower impact velocity (45 m/s), higher stand-off distance (240 mm) and higher impingement angle (90°), it can be seen that in the second case the breaking of glass fibers is more prominent (Fig. 11). It appears that cracks have grown on the fibers giving rise to breaking of the fibers into small fragments. Further the cracks have been annihilated at the fiber matrix interface and seem not to have penetrated through the matrix. Change in impact angle from oblique to normal changes the topography of the damaged surface very significantly. Figure 11 shows the dominance of

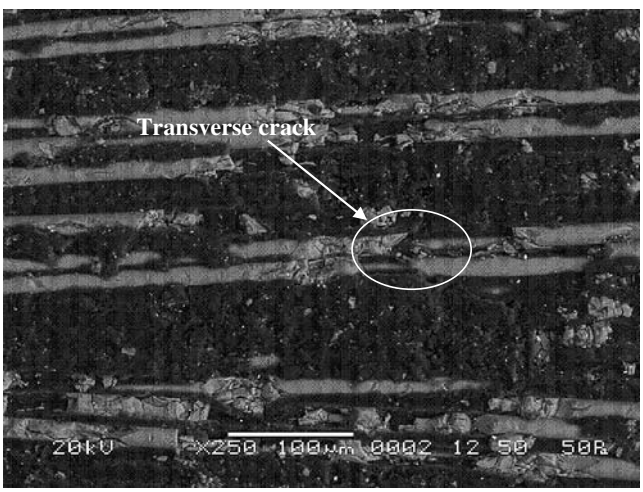

Fig. 9 SEM micrograph (× 250) of GF Polymer composite eroded surface (impact velocity 58 m/s, fiber loading 50%, S.O.D 120 mm, impingement angle 60° and erodent size 300 μm)

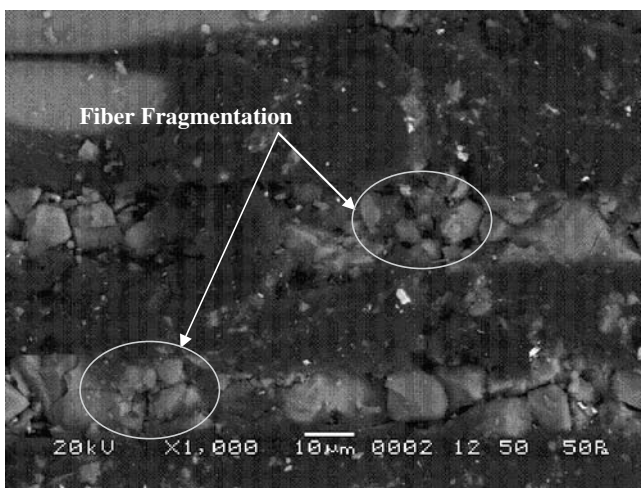

Fig. 11 SEM micrograph (× 1,000) of GF Polymer composite eroded surface (impact velocity 45 m/s, fiber loading 50%, S.O.D 240 mm, impingement angle 90° and erodent size 800 μm)

micro-chipping and micro-cracking phenomena. It can be seen that multiple cracks originate from the point of impact, intersect one another and form wear debris due to brittle fracture in the fiber body. After repetitive impacts, the debris in platelet form are removed and account for the measured wear loss. The occurrence of peak erosion rate at 60° impact is understandable. In this case, both abrasion and erosion processes play important roles. The sand particles after impacting, slide on the surface and abrade while dropping down. The wear and subsequently the damage are therefore more than that in the case of normal impact. Marks of micro-ploughing on the ductile polyester matrix region seen in Fig. 10 support this argument.

Polyester is a thermoplastic polymer and it is known that it shows a ductile erosion response. So a possible reason for the semi-ductile erosion behavior exhibited by the polyester based composites in the present investigation is that the glass fibers used as reinforcements are a typical brittle material. Their erosion is caused mostly by damage mechanism such as micro-cracking. Such damage is supposed to increase with the increase of kinetic energy loss of the impinging sand particles. According to Hutchings et al. [27] the kinetic energy loss is a maximum at normal impact, where erosion rates are highest for brittle materials. In the present study also, the peak erosion rate shifts to impingement angle (60°) and it is clearly due to the brittle nature of glass fibers. So although polyester is a ductile material, the presence of fibers makes the composite relatively more sensitive to impact energy which increases when the impact mode pattern changes from tangential (α= 0°) to normal (α=90°). This explains the semi-ductile nature of the glass–polyester composites with respect to solid particle erosion.

From Table 4, the overall mean for the *S*/*N* ratio of the erosion rate is found to be −48.97 dB. Figure 12 shows graphically the effect of the six control factors on erosion rate. The analysis was made using the popular software specifically used for design of experiment applications known as MINITAB 14. Before any attempt is made to use this simple model as a predictor for the measures of performance, the possible interactions between the control factors must be considered. Thus factorial design incorporates a simple means of testing for the presence of the interaction effects.

Analysis of the result leads to the conclusion that factor combination of A_1, B_2, C_1, D_1 and E_2 gives minimum

Table 4 Experimental design using L_{27} orthogonal array

Experiment. no.	Impact velocity (*A*) (m/s)	Fiber loading (*B*) (%)	Stand-off distance (*C*) (mm)	Impingement angle (*D*) (degree)	Erodent size (*E*) (μm)	Erosion rate (E_r) mg/kg	*S*/*N* Ratio (dB)
1	32	30	120	30	300	309.83	−49.8225
2	32	30	180	60	500	315.25	−49.9731
3	32	30	240	90	800	305.19	−49.6914
4	32	40	120	60	500	186.07	−45.3936
5	32	40	180	90	800	272.79	−48.7166
6	32	40	240	30	300	230.96	−47.2707
7	32	50	120	90	800	287.69	−49.1785
8	32	50	180	30	300	279.85	−48.9385
9	32	50	240	60	500	255.25	−48.1393
10	45	30	120	60	800	288.86	−49.2137
11	45	30	180	90	300	249.80	−47.9518
12	45	30	240	30	500	255.25	−48.1393
13	45	40	120	90	300	239.76	−47.5955
14	45	40	180	30	500	249.18	−47.9304
15	45	40	240	60	800	298.23	−49.4910
16	45	50	120	30	500	261.17	−48.3385
17	45	50	180	60	800	364.31	−51.2294
18	45	50	240	90	300	389.94	−51.8201
19	58	30	120	90	500	315.10	−49.9690
20	58	30	180	30	800	245.19	−47.7901
21	58	30	240	60	300	219.89	−46.8441
22	58	40	120	30	800	261.27	−48.3418
23	58	40	180	60	300	239.76	−47.5955
24	58	40	240	90	500	210.66	−46.4716
25	58	50	120	60	300	369.47	−51.3516
26	58	50	180	90	500	452.81	−53.1183
27	58	50	240	30	800	391.45	−51.8535

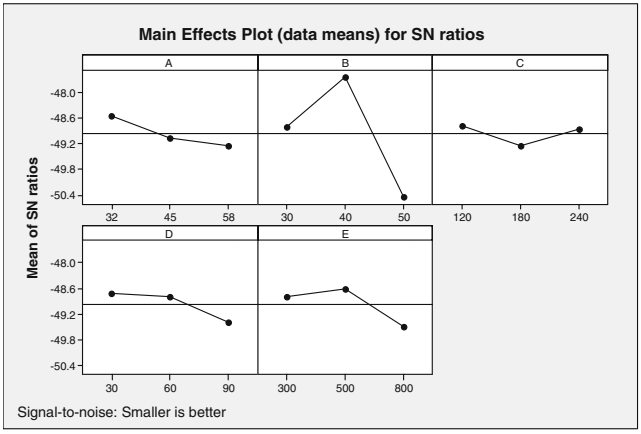

Fig. 12 Effect of control factors on erosion rate

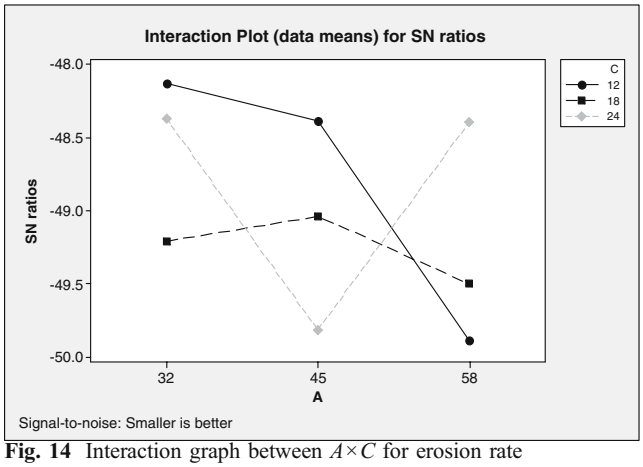

Fig. 14 Interaction graph between $A \times C$ for erosion rate

erosion rate. The interaction graphs are shown in Figs. 13, 14 and 15. As for as minimization of erosion rate is concerned, factor B and E have significant effect whereas factor C has least effect. It is observed from Fig. 13 that the interaction between $A \times B$ shows most significant effect on erosion rate. But the factor C individually has less contribution on output performance, and their combination of interaction with factor A and B ($A \times C$ and $B \times C$) is shown in Figs. 14 and 15 can be neglected for further study.

Erosion efficiency

The hardness alone is unable to provide sufficient correlation with erosion rate, largely because it determines only the volume displaced by each impact and not really the volume eroded. Thus a parameter which will reflect the efficiency with which the volume that is displaced is removed should be combined with hardness to obtain a better correlation. The erosion efficiency is obviously one such parameter. This thought has already been reflected in the theoretical model but the evaluation of erosion efficiency can be made only on the basis of experimental data. Hence, the values of erosion efficiencies of these composites calculated using Eq. 2 are summarized in Table 5 along with their hardness values and operating conditions. It clearly shows that erosion efficiency is not exclusively a material property; but also depends on other operational variables such as impingement angle and impact velocity. The erosion efficiencies of these composites under normal impact (η_{normal}) vary from 3 to 6%, 6–9% and 9–12% for impact velocities 58, 45 and 32 m/s respectively. The value of η for a particular impact velocity under oblique impact can be obtained simply by multiplying a factor $1/\sin^2\alpha$ with η_{normal}. Similar observation on velocity dependence of erosion efficiency has previously been reported by few investigators Roy et al. [28], and Arjula and Harsha [29].

The theoretical erosion wear rate (E_{rth}) of the polyester-GF composites are calculated using Eq. 7. These values are compared with those obtained from experiments (E_{rexpt}) conducted under similar operating conditions. Seventy five percent of data collected from erosion test is used for

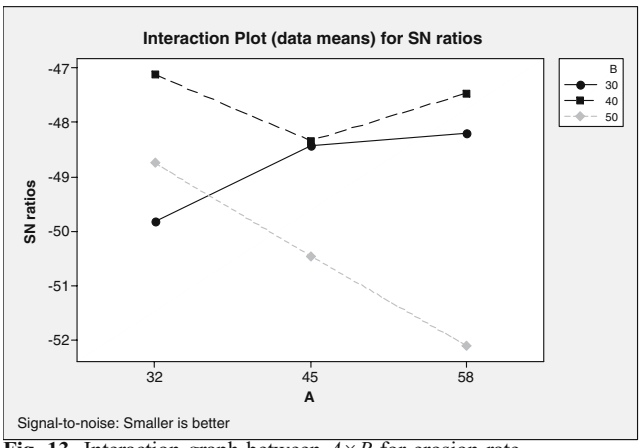

Fig. 13 Interaction graph between $A \times B$ for erosion rate

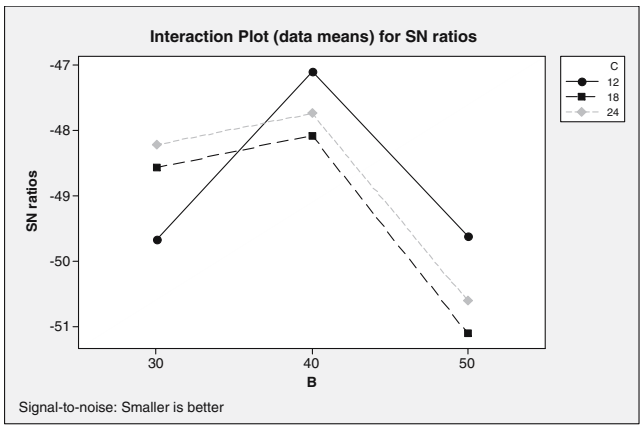

Fig. 15 Interaction graph between $B \times C$ for erosion rate

Table 5 Erosion efficiency of GF-reinforced polyester resin

Experiment. no.	Impact velocity (V) m/s	Density of eroding material (ρ) kg/m^3	Hardness of eroding material (H_v) MPa	Erosion rate (E_r) mg/kg	Erosion efficiency (η)
1	32	1738	32	309.83	43.70689
2	32	1738	32	315.25	12.83002
3	32	1738	32	305.19	10.76308
4	32	1874	34	186.07	7.462042
5	32	1874	34	272.79	9.479905
6	32	1874	34	230.96	32.10497
7	32	1932	39	287.69	11.12368
8	32	1932	39	279.85	43.28217
9	32	1932	39	255.25	11.38925
10	45	1738	32	288.86	5.944763
11	45	1738	32	249.80	4.454857
12	45	1738	32	255.25	18.2082
13	45	1874	34	239.76	4.213347
14	45	1874	34	249.18	17.51554
15	45	1874	34	298.23	6.047942
16	45	1932	39	261.17	20.42593
17	45	1932	39	364.31	8.22007
18	45	1932	39	389.94	7.624237
19	58	1738	32	315.10	3.382663
20	58	1738	32	245.19	10.52866
21	58	1738	32	219.89	2.724091
22	58	1874	34	261.27	11.05526
23	58	1874	34	239.76	2.926861
24	58	1874	34	210.66	2.228443
25	58	1932	39	369.47	5.018254
26	58	1932	39	452.81	5.329466
27	58	1932	39	391.45	18.42909

training whereas 25% data is used for testing. The parameters of three layer architecture of ANN model are set as input nodes=5, output node=1, hidden nodes=12, learning rate=0.01, momentum parameter=0.03, number of epochs=200,000 and a set of predicted output (E_{rANN}) is obtained. Table 6 presents a comparison among the theoretical, experimental and the ANN predicted results. The errors calculated with respect to the theoretical results are also given. It is observed that maximum error between theoretical and experimental wear rate is 0–10%, whereas same between ANN prediction and experimental wear rate is 0–14%. The error in case of ANN model can further be reduced if number of test patterns is increased. However, present study demonstrates application of ANN for prediction of wear rate in a complex process of solid particle erosion of polymer composites.

The magnitude of η can be used to characterize the nature and mechanism of erosion. For example, ideal microploughing involving just the displacement of the material from the crater without any fracture (and hence no erosion) will results in η=0. In contrast, if the material removal is by ideal micro-cutting, η=1.0 or 100%. If erosion occurs by lip or platelet formation and their fracture by repeated impact, as is usually the case in the case of ductile materials, the magnitude of η will be very low, i.e. $\eta \leq 100\%$. In the case of brittle materials, erosion occurs usually by spalling and removal of large chunks of materials resulting from the interlinking of lateral or radial cracks and thus η can be expected to be even greater than 100% [29]. According to the categorization made by Roy et al. [28], the erosion efficiencies of the composites under the present study indicate that at low impact speed the erosion response is semi-ductile (η=10–100%). On the other hand at relatively higher impact velocity the composites exhibit ductile (η<10%) erosion behavior.

ANOVA and the effects of factors

In order to understand a concrete visualization of impact of various factors and their interactions, it is desirable to develop analysis of variance (ANOVA) table to find out the order of significant factors as well as interactions. Table 7 shows the results of the ANOVA with the erosion rate. This analysis was undertaken for a level of confidence of significance of 5%. The last column of the table indicates that the main effects are highly significant (all have very small p values).

Table 6 Comparison of theoretical, experimental and ANN results

Experiment no.	E_{rth} (mg/kg)	$E_{rexpt.}$ (mg/kg)	E_{rANN} (mg/kg)	Error (%) ($E_{rth}-E_{rexpt}$)	Error (%) ($E_{rth}-E_{rANN}$)
1	314.84	309.83	340.33	1.5912	8.0945
2	321.69	315.25	308.95	2.0019	3.9601
3	304.17	305.19	291.93	0.3353	4.0226
4	201.98	186.07	176.31	7.8765	12.711
5	271.78	272.79	295.34	0.3716	8.6687
6	238.45	230.96	269.54	3.1411	13.038
7	286.69	287.69	251.33	0.3488	12.332
8	296.75	279.85	258.51	5.6950	12.886
9	276.81	255.25	292.07	7.7887	5.5125
10	309.29	288.86	289.53	6.6054	6.3882
11	248.76	249.80	267.10	0.4180	7.3727
12	266.73	255.25	238.76	4.3039	10.485
13	238.76	239.76	233.65	0.4188	2.1385
14	257.34	249.18	251.49	3.1693	2.2722
15	319.46	298.23	321.04	6.6455	0.4947
16	289.38	261.17	293.27	9.7484	1.3438
17	378.38	364.31	327.33	3.7184	13.491
18	387.95	389.94	351.06	0.5155	9.5067
19	314.14	315.10	272.29	0.3056	13.321
20	259.21	245.19	248.82	5.4087	4.0069
21	227.76	219.89	206.00	3.4553	9.5529
22	281.37	261.27	318.62	7.1436	13.239
23	248.75	239.76	277.37	3.6140	12.312
24	209.66	210.66	229.48	0.4769	9.4519
25	387.34	369.47	349.40	4.6135	9.7947
26	451.81	452.81	391.23	0.2213	13.408
27	405.27	391.45	363.25	3.4101	10.369

From Table 7, one can observe that the fiber loading (p=0.004), erodent size (p=0.145), impingement angle (p=0.252) and impact velocity (p=0.265) have great influence on erosion rate. The interaction of impact velocity × fiber loading (p=0.029) shows significance of contribution on the erosion rate and the factor stand-off distance (p=0.493) and impact velocity × stand-off distance (p=0.150), fiber loading × stand-off distance (p=0.162) present less significance of contribution on erosion rate.

Table 7 ANOVA table for erosion rate

Source	*df*	Seq SS	Adj SS	Adj MS	*F*	*P*
A	2	2.3056	2.3056	1.1528	1.88	0.265
B	2	35.4646	35.4646	17.7323	28.95	0.004
C	2	1.0737	1.0737	0.5369	0.88	0.483
D	2	2.4297	2.4297	1.2149	1.98	0.252
E	2	3.9765	3.9765	1.9882	3.25	0.145
A×*B*	4	21.5781	21.5781	5.3945	8.81	0.029
A×*C*	4	7.5740	7.5740	1.8935	3.09	0.150
B×*C*	4	7.1630	7.1630	1.7908	2.92	0.162
Error	4	2.4498	2.4498	0.6125		
Total	26	84.0150				

Confirmation experiment

The confirmation experiment is the final test in the design of experiment process. The purpose of the confirmation experiment is to validate the conclusions drawn during the analysis phase. The confirmation experiment is performed by conducting a new set of factor settings $A_2B_3D_2E_3$ to predict the erosion rate. The estimated *S*/*N* ratio for erosion rate can be calculated with the help of following prediction equation:

$$\begin{aligned}\widehat{\eta}_1 &= \overline{T} + (\overline{A}_2 - \overline{T}) + (\overline{B}_3 - \overline{T}) \\ &\quad + [(\overline{A}_2\overline{B}_3 - \overline{T}) - (\overline{A}_2 - \overline{T}) - (\overline{B}_3 - \overline{T})] \\ &\quad + (\overline{D}_2 - \overline{T}) + (\overline{E}_3 - \overline{T}) \end{aligned} \quad (9)$$

$\overline{\eta}_1$ Predicted average
$\overline{T}$ Overall experimental average
$\overline{A}_2$, $\overline{B}_3$, $\overline{D}_2$ and $\overline{E}_3$ Mean response for factors and interactions at designated levels.

By combining like terms, the equation reduces to

$$\overline{\eta}_1 = \overline{A}_2\overline{B}_3 + \overline{D}_2 + \overline{E}_3 - 2\overline{T} \quad (10)$$

A new combination of factor levels A_2, B_3, D_2 and E_3 is used to predict deposition rate through prediction equation and it is found to be $\overline{\eta}_1 = -50.8283$ dB. For each performance measure, an experiment was conducted for a different factors combination and compared with the result obtained from the predictive equation as shown in Table 8.

The resulting model seems to be capable of predicting erosion rate to a reasonable accuracy. An error of 2.48% for the *S/N* ratio of erosion rate is observed. However, the error can be further reduced if the number of measurements is increased. This validates the development of the mathematical model for predicting the measures of performance based on knowledge of the input parameters.

Factor settings for minimum erosion rate

In this study, an attempt is made to derive optimal settings of the control factors for minimization of erosion rate. The single-objective optimization requires quantitative determination of the relationship between erosion rates with combination of control factors. In order to express, erosion rate in terms of mathematical model in the following form is suggested.

$$\mathrm{Er} = K_0 + K_1 \times A + K_2 \times B + K_3 \times D + K_4 \times E + K_5 \times A \times B \tag{11}$$

Here, E_r is the performance output terms and K_i (i=0, 1……..5) are the model constants. The constant are calculated using non-linear regression analysis with the help of SYSTAT 7 software and the following relations are obtained.

$$E_r = 1.521 - 1.633A - 1.387B + 0.088D + 0.078E + 1.221AB \tag{12}$$

$$r^2 = 0.98$$

The correctness of the calculated constants is confirmed as high correlation coefficients (r^2) in the tune of 0.96 are obtained for Eq. 1 and therefore, the models are quite suitable to use for further analysis. Here, the resultant objective function to be maximized is given as:

$$\text{Maximize } Z = 1/f \tag{13}$$

f Normalized function for erosion rate

Subjected to constraints:

$$A_{\min} \le A \le A_{\max} \tag{14}$$

$$B_{\min} \le B \le B_{\max} \tag{15}$$

$$D_{\min} \le D \le D_{\max} \tag{16}$$

$$E_{\min} \le E \le E_{\max} \tag{17}$$

The min and max in Eqs. (14) to (17) shows the lowest and highest control factors settings (control factors) used in this study (Table 2).

Genetic algorithm (GA) is used to obtain the optimum value for single-objective outputs to optimize the single-objective function. The computational algorithm is implemented in Turbo C^{++} and run on an IBM Pentium IV machine. Genetic algorithms (GAs) are mathematical optimization techniques that simulate a natural evolution process. They are based on the Darwinian Theory, in which the fittest species survives and propagate while the less successful tend to disappear. Genetic algorithm mainly depends on three types of operators viz., reproduction, crossover and mutation. Reproduction is accomplished by copying the best individuals from one generation to the next, what is often called an elitist strategy. The best solution is monotonically improving from one generation to the next. The selected parents are submitted to the crossover operator to produce one or two children. The crossover is carried out with an assigned probability, which is generally rather high. If a number randomly sampled is inferior to the probability, the crossover is performed. The genetic mutation introduces diversity in the population by an occasional random replacement of the individuals. The mutation is performed based on an assigned probability. A

Table 8 Results of the confirmation experiments for erosion rate

	Optimal control parameters prediction	experimental
Level	A_2 $B_3D_2E_3$	A_2 $B_3D_2E_3$
S/N ratio for Erosion rate (dB)	−50.8283	−49.5677

Table 9 Optimum conditions for performance output

Control factors and performance characteristics	Optimum conditions
A: Impact velocity (m/s)	33.15
B: Fiber loading (%)	41.02
D: Impingement angle (degree)	59.45
E: Erodent size (μm)	500.0
Erosion rate (mg/kg)	364.72

random number is used to determine if a new individual will be produced to substitute the one generated by crossover. The mutation procedure consists of replacing one of the decision variable values of an individual while keeping the remaining variables unchanged. The replaced variable is randomly chosen and its new value is calculated by randomly sampling within its specific range. In genetic optimization, population size, probability of crossover and mutation are set at 50, 75, and 5% respectively for all the cases. Number of generation is varied till the output is converted. Table 9 shows the optimum conditions of the control factors with optimum performance out put gives a better combination of set of input control factors.

Conclusions

This analytical and experimental investigation into the erosion behavior of glass fiber reinforced polyester composites leads to the following conclusions:

1. Conservation of energy principle is applied to the multiple impact erosion process and consequently a mathematical model based on ductile mode erosion is developed. To overcome the shortcomings of existing theoretical models 'erosion efficiency' term has been introduced. It has been demonstrated that if supported by an appropriate magnitude of erosion efficiency, the model performs well for polyester matrix composites for normal as well as oblique impacts.
2. Solid particle erosion characteristics of these composites can be successfully analyzed using Taguchi experimental design scheme. Taguchi method provides a simple, systematic and efficient methodology for the optimization of the control factors. This approach not only needs engineering judgment but also requires a rigorous mathematical model to obtain optimal process settings.
3. The results indicate that erodent size, fiber loading, impingement angle and impact velocity are the significant factors in a declining sequence affecting the erosion wear rate. Although the effect of impact velocity is less compared to other factors, it cannot be ignored because it shows significant interaction with fiber loading. An optimal parameter combination is determined, which leads to minimization of material loss due to erosion.
4. The composites exhibit semi-ductile erosion characteristics with the peak erosion wear occurring at 60° impingement angle. This nature has been explained by analyzing the possible damage mechanism with the help of SEM micrographs. It is concluded that the inclusion of brittle fibers in ductile polyester matrix is responsible for this semi-ductility.
5. The erosion efficiency (η) values obtained experimentally also suggest that the glass fiber reinforced polyester composites exhibit semi-ductile erosion response (η=10–60%) for low impact velocities. However, for relatively high impact velocity, they present a ductile erosion response (η<10%).
6. Two predictive models based on ANN approach is proposed. It is demonstrated that that these models well reflect the effects of various factors on the erosion loss and their predictive results are consistent with experimental observations.
7. The rationale behind the use of genetic algorithm lies in the fact that genetic algorithm has the capability to find the global optimal parameter settings whereas the traditional optimization techniques are normally stuck up at the local optimum values. The optimum settings are found to be impact velocity=33.15 m/s, fiber loading=41.02%, impingement angle=59.45°, erodent size=500.0 μm, and resulting erosion rate=364.72 mg/kg as far as present experimental conditions are concerned.
8. This work leaves wide scope for future investigators to study the erosion behavior of such composites with short fiber reinforcement and with particulate filling.

References

1. Wahl H, Hartenstein F (1946) Strahlverschleiss, Frankh'sche Verlagshandlung, Stuttgart
2. Bitter JGA (1963) Wear 6:169–190
3. Raask E (1968) Wear 13:303–313
4. Hibbert WA, Roy J (1965) Aero Soc 69:769–776
5. Pool KV, Dharan CKH, Finnie I (1986) Wear 107:1–12
6. Kulkarni SM, Kishore (2001) Polym Polym Compos 9:25–30
7. Ruff AW, Ives LK (1975) Wear 35:195–199
8. Barkoula NM, Karger-Kocsis J (2002) Wear 252:80–87
9. Tewari US, Harsha AP, Hager AM, Friedrich K (2002) Wear 252:992–1000
10. Häger A, Friedrich K, Dzenis YA, Paipetis SA (1995) Proceedings of the ICCM-10, Canada Wood head Publishing Ltd., Cambridge, pp 155–162
11. Miyazaki N, Takeda T (1993) J Compos Mater 27:21–31
12. Tilly GP, Sage W (1970) Wear 16:447–465
13. Lindsley BA, Marder AR (1999) Wear 225:510–516
14. Sundararajan G, Manish R (1997) Tribol Int 30:339–359
15. Mahapatra SS, Patnaik A (2006) Solid Waste Technol Manag 32 (1):28–35
16. Mahapatra SS, Patnaik A (2006) Indian J Eng Mater Sci 13:493–502
17. Mahapatra SS, Patnaik A (2006) Int J Adv Manuf Technol DOI 10.1007/s00170-006-0672-6
18. Mahapatra SS, Patnaik A (2007) J Braz Soc Mech Sci 28(4):423–430
19. Mahapatra SS, Patnaik A (2006) Inst Eng 87:16–24
20. Mahapatra SS, Patnaik A (2006) The International Journal for Manufacturing Science and Technology 8(1):5–12

21. Mahapatra SS, Patnaik A (2007) The International Journal for Manufacturing Science and Technology 9(2):129–144
22. Mishra PK (1997) Narosa, New Delhi
23. Glen SP (1993) Addison-Wesley, New York
24. Madhav SP (1989) Prentice-Hall, Eaglewood Cliffs, NJ.
25. Harsha AP, Tewari US, Venkatraman B (2003) Wear 254:693–712
26. Sundararajan G, Roy M, Venkataraman B (1990) Wear 140:369–381
27. Hutchings IM, Winter RE, Field JE (1976) Proc Roy Soc Lond Ser A 348:379–392
28. Roy M, Vishwanathan B, Sundararajan G (1994) Wear 171:149–161
29. Arjula S, Harsha AP (2006) Polym test 25:188–196